Vibrational Energy Scavenging: An Interdisciplinary Engineering Design Project

By:

Jeff Wolchok[1]
Jessica Moffitt[2]
Jennifer van Rij[2]

[1] Department of Bioengineering
[2] Department of Mechanical Engineering
University of Utah
Salt Lake City, Utah

Introduction:
IGERT is an NSF-wide program intended to meet the challenges of educating Ph.D. scientists and engineers with the multidisciplinary backgrounds and the technical, professional, and personal skills needed for the career demands of the future. The program is intended to catalyze a cultural change in graduate education by establishing new, innovative models for graduate education and training in a fertile environment for collaborative research that transcends traditional disciplinary boundaries.

The Utah Integrative Graduate Education and Research Training (IGERT) award supported the establishment of a multidisciplinary graduate training program of education and research on extremely small scale thermal-fluid systems. The applications of extremely small scale thermal- and fluid-systems are expanding exponentially, including: silicon microfabrication technology based turbines; microscale heat exchangers for cooling high-power electronics, and micro- and nano- scale chemical and biological analyses systems. The objective of this program is to create the first integrated, multidisciplinary educational program in extremely small scale thermal-fluid systems. An interdisciplinary faculty will provide a comprehensive education and research training program, including six new, specialized courses and integrated research experiences. These classes will involve a diverse set of topics such as scaling issues, micromachining, interfacial phenomena, and thin-film energy transport. The students will participate in formal classroom and laboratory training, industrial and government laboratory internships, a monthly interdisciplinary seminar, and international educational experiences.

Throughout the duration of the fellowship students participated in small group (3-4 members) projects that were intended to complement the coursework. Projects were microsystems focused and designed to encourage the involvement of an interdisciplinary design team. Project progression was intended to track with the coursework with the goal of applying class learning to a complex project with no clear solution. The coursework and projects were intended to emphasize (1) the fundamental engineering physics and chemistry that are important at these small scales; (2) fabrication technologies; (3) design for manufacturing; and (4) testing and analysis of complete systems. Our group was interested in microscale energy conversion, and over the course of the semester refined our project to look specifically at vibrational energy conversion. In this paper we will review the microsystems and communication coursework that was required of all IGERT students, discuss the associated design project, and provide student based recommendations that may be used to refine future programs.

Coursework:
Graduate students accepted into the IGERT program were required to complete three semester length microsystems courses. Courses were taken in series, with the experience gained in one course intended to build upon the next. In conjunction with the technical courses, enrollment in a once a week short course in communication was expected. Although the microsystems courses were open to all students, communication course enrollment was limited to IGERT students. The fall 2003 IGERT class consisted of 12 students with undergraduate backgrounds that included materials, mechanical, electrical, chemical, biomedical, and computer engineering.

The first technical course taken in the series was entitled “Fundamentals of Microscale Engineering”. The course was designed to introduce students to the field and covered a broad

range of topics including scaling laws, microfabrication technologies, metrology techniques, thermal fluid phenomena, and applications. The concurrent communication short course was designed to explore creativity and the design process. It was during this first semester that design teams were formed from the IGERT students. The groups which consisted of 3 to 4 students were expected to initially select a broad topic and use the creativity tools and technical knowledge learned during the semester to further refine our design topic.

The second course was entitled "Fundamentals of Micromachining" and focused primarily on microfabrication techniques. The class included a weekly lab section which introduced students to the various microfabrication techniques available in the University of Utah Microfabrication Facility. The second semester communication short course focused on teamwork. Student groups worked towards refining their project and developing a fabrication process. Where appropriate, modeling and simulation work was also accomplished.

The third course in the series "Microsystems Design and Characterization" was designed to generalize microsystems design considerations with practical emphasis on MEMS and IC characterization and physical analysis. Specific emphasize was placed on (1) designing for reliability; (2) performance characterization; (3) physical characterization; and (4) implementation of feedback loops in the design process. The coursework was supplemented by laboratory exercises. At this stage in the coursework a working prototype should be fabricated and available for characterization. Ideally, characterization and testing results would lead to design improvements. Design improvement could then be incorporated into a second generation prototype. Oral and written reports were expected.

Design Project:

The shift towards low power wireless sensing devices creates an opportunity for novel energy sources. Traditionally, wireless devices are powered by either rechargeable or non-rechargeable batteries. While very reliable, all batteries have a limited lifetime and require repeated access to the device for recharge or replacement. As an alternative, non-traditional microscale energy sources could be harnessed to provide the necessary energy. This has become possible because of the recent advances in integrated circuit fabrication which have reduced the power needs of many wireless sensors down to the milliwatt range [1].

Promising sources of renewable energy, mechanical vibrations, are present all around us. These vibrations are commonplace wherever mechanical machinery is operating (homes, office building, vehicles, etc.) and could theoretically provide enough energy to power microdevices. There are three methods that can be used to convert mechanical vibrations into electrical energy; 1) electromagnetic, 2) electrostatic, 3) piezoelectric conversion. Electromagnetic power conversion results from the relative motion of an electrical conductor in a magnetic field. Electrostatic conversion occurs as two conductors separated by a dielectric move in relation to one another resulting in a change in capacitance. The last method, piezoelectric conversion, occurs whenever piezoelectric materials are physically deformed and a charge separation is produced. Each of the conversion methods requires input energy in the form of motion to drive the process. The motion can be supplied by mechanical vibrations, thereby providing a renewable source of energy and enabling battery free operation of low power microdevices.

The devices which have shown the greatest potential use the electrostatic conversion process [1]. The device utilizes an electrostatic comb drive that is operated as a generator rather than an actuator. When exposed to mechanical vibrations the capacitance of the comb drive cycles between a maximum and minimum in sync with the vibrations. The power generated by the device is proportional to the change in capacitance and the frequency at which it is vibrated. The range of capacitances possible and the frequencies to which the device will respond are affected by the geometry. As a result it is possible to design the device such that it is optimized for specific frequencies.

Electromechanical Modeling:
To simulate the physical system a mass and spring model is used to describe the transfer of ambient vibration kinetic energy to a vibrating mass (Fig 1).

$$m\ddot{z} + f_e(z) + f_m(\dot{z}) + kz = -m\ddot{y} \qquad (1)$$

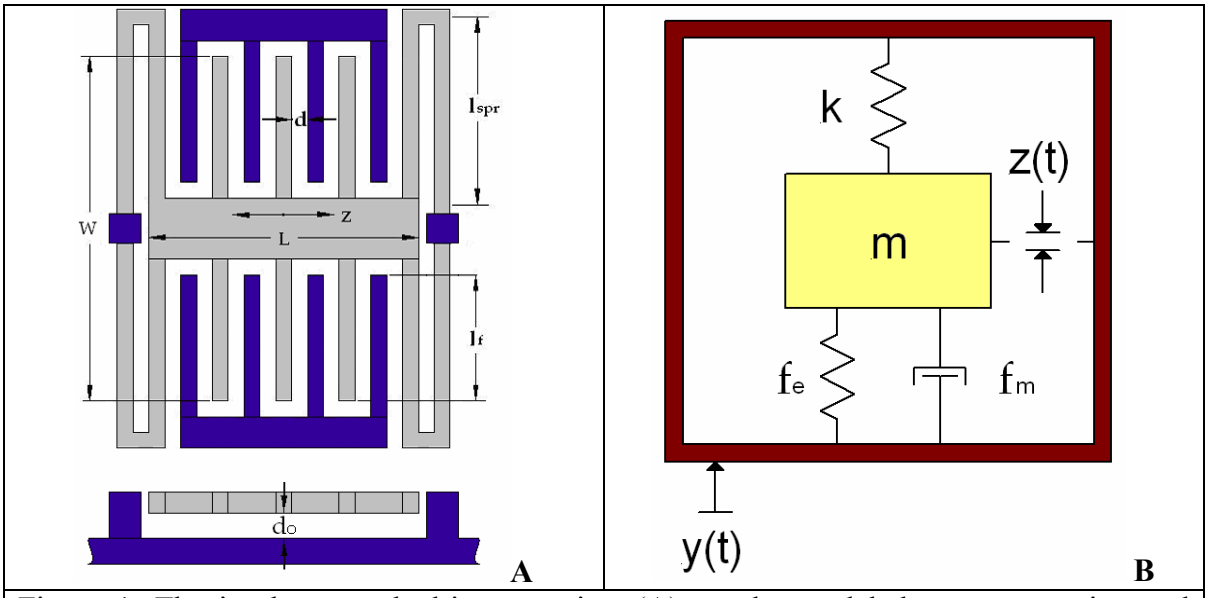

Figure 1. The in-plane comb drive capacitor (A) can be modeled as mass, spring and damper system (B).

The in-plane gap closing converter (Fig 1) converts ambient vibrational energy into electrical energy by operating as a charge constrained variable capacitor [10]. The net energy (ΔU) converted per vibration cycle is proportional to the change in capacitance.

$$\Delta U = \frac{V_o V_{\max}}{2}\left(C_{\max} - C_{\min}\right) \qquad (2)$$

The power gain per cycle can be predicted if the maximum and minimum capacitances of the system are known. These values can be calculated based solely on the geometric design and physical constants of the system. Combined models of the physical and electrostatic systems are used to optimize the design.

$$C_{\min} = \frac{2N_g \varepsilon_0 L_f h}{d} \quad (3)$$

$$C_{\max} = N_g \varepsilon_0 L_f h \left(\frac{2d}{d^2 - z_{\max}^2} \right) \quad (4)$$

Where, Ng is the number of gaps per side; ε0 is the dielectric constant of free space; Lf is the over lapping length of the fingers; h is the thickness of the device; d is the nominal gap between fingers; and zmax is the displacement of the shuttle at the mechanical stops. By combining the kinetic (eq. 1) electrostatic models (eq. 2-4) the natural frequency of the system and its power output, can be determined and optimized numerically.

Based on the analytical conversion process described, a numerical model of the energy scavenger was created in MATLAB. The numerical model couples the electrical and mechanical interactions by approximating the kinetic model as a finite difference equation and solving for position (z). Using the model's predictions for vibration frequency, capacitance, displacement, and power output the energy scavenging system was optimized based on several constraints. First, for maximum output the system must be designed such that its natural frequency, ωn, matches the ambient vibration frequency, ω. And, because the power output is proportional to 1/ω, the system was modeled for low ambient vibrations of 120 Hz. Second, a large change of capacitance, meaning an increase in power output, can be obtained by reducing the gap between the fingers, increasing the device thickness, elongating the fingers, and increasing the length of the shuttle mass. However, the minimum gap and maximum aspect ratio are limited by our fabrication process to 15μm and 3 respectively. Additionally, the length of the fingers, the size of the shuttle mass, and the spring dimensions can not be changed independently without changing the vibration mode of the system. Based on these considerations the numerical modeling results, as well as some of the parameters used to obtain these results, are given Table I.

Table I - Device Parameters and Outputs

Variable	Description	Value	
Pout	Output power	7	μW
Cmax	Maximum capacitance	157	pF
Cmin	Minimum capacitance	53	pF
Vmax	Maximum voltage	10	V
Vo	Input voltage	5	V
d	Nominal gap between fingers	15	μm
L	Length of shuttle mass	10	mm
Lf	Length of fingers	3	mm
Lspr	Length of folded spring	0.55	mm
t	Device thickness	45	μm
W	Width of shuttle mass	8	mm
zmax	Maximum displacement	12.2	μm
ω	Operating frequency	120	Hz

Circuit Design:
A critical aspect of system operation deals with timing the opening and closing of the switches. For optimal energy conversion to take place, switch SW1 in Figure 2 should close when the capacitance is at its peak value, corresponding to the point when the gap between fingers is the smallest. This ensures that the variable capacitor collects the maximum possible charge. To optimize charge collection on the storage capacitor, switch SW2 should close when the capacitance is minimized, corresponding to a large gap between fingers. To control this portion of the system, a circuit will be implemented that will sense the capacitive state of the device and close the proper switch accordingly.

When both switches are open, charge is trapped on the variable capacitor. If the capacitor is allowed to oscillate while charge is constrained, the drop in capacitance from Cmax to Cmin will cause a corresponding increase in voltage. Refer to the first box in Figure 2 for a graphical representation. This varying voltage will be the input, Vin, to the control circuit, and the means for monitoring the capacitive state of the device. When the device is exposed to constant vibration, this voltage will likely take the form of a sinusoid with relatively constant frequency.

To physically implement each of the switches, the source-to-drain region of an n-type MOSFET will be placed in series with a diode oriented to allow current flow from left to right in Figure 2. The gates of each MOSFET will allow current to pass when the proper voltage is applied, and the diodes will prevent charge from leaking back to the supply voltage in the case of SW1, or from escaping the storage capacitor in the case of SW2.

A comparator known as a Schmitt Trigger will be used to translate the sinusoidal input voltage into short pulses suitable for activating the gates of the MOSFET switches (Fig 2).

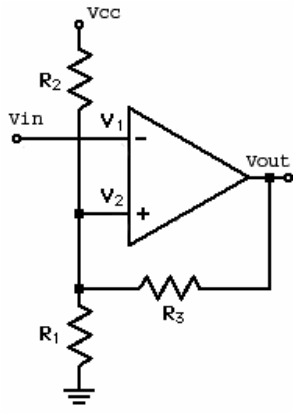

Figure 2: Schmitt Trigger

When the input voltage in the above circuit goes above or below a specific reference point, the output switches between the positive and negative rail voltages accordingly. The reference voltage V2 is set according to resistor values as shown in (5) and (6).

$$V_2 = R_{eq}\left(\frac{1}{R_2} + \frac{1}{R_3}\right)V_{CC} \quad (5)$$

$$R_{eq} = R_1 \| R_2 \| R_3 \quad (6)$$

The feedback loop slightly alters the reference voltage to compensate for noise in the incoming signal. By selecting a reference voltage that is very close to the peak voltage of the input, it is possible to create very short pulses at the output.

The voltage pulses created by the Schmitt Trigger will correspond to the peaks of the input voltage (minimum capacitance), and can be used to operate switch SW2 directly. To operate the remaining switch, a phase shifter circuit (Fig. 3) will be used to shift the pulses by 90 degrees to match the valleys of the input voltage (maximum capacitance).

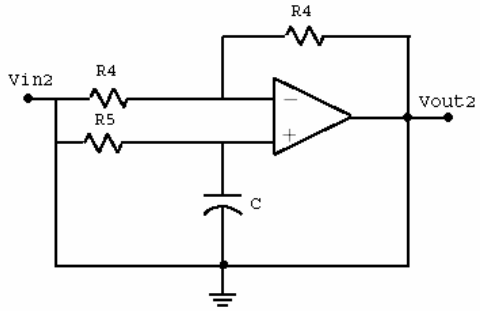

Figure 3: Phase Shifter

The ratio of the two resistors labeled R4 determines the gain, which is 1 for this application. The values of the capacitor and resistor R5 determine the amount of phase shift. A 90 degree phase shift is obtained by selecting component values as shown in (14) for a specific chosen frequency fo, which will correspond to the frequency of vibration.

$$f_o = \frac{1}{2\pi R_5 C} \quad (7)$$

Characterizing the system prototype can be done using a breadboard with discrete components. By soldering wires to bond pads on the device it will be possible to establish an initial charge and sample the voltages associated with oscillation. Preliminary testing can be done by exposing the comb drive to various vibration sources to verify the steady state frequency found through simulation. Initial results will provide the opportunity to adjust component values and reevaluate control circuit performance.

Eventually the control circuitry will need to be fabricated and integrated with the comb drive into an inclusive package. The available software program CADENCE provides a complete set of tools for circuit design, verification, and layout design, and can be used in future work by generating masks for fabrication. Work done in this area would include designing transistor-level op-amps with the proper dimensions and integrating them with the other elements of the control circuitry.

Test Structures:
In an effort to produce a high quality device, as well as to characterize the process and the device itself, several test structures will be incorporated into the fabrication process. The measurements proposed in this section are expected to enable in situ process monitoring and facilitate prompt identification of device defects. Specifically, measurements of layer stress, feature geometry, elastic modulus, natural frequency, sheet resistance and adhesion are described in this section (Table II).

Table II. Electrostatic energy converter fabrication tests.

Layer	Quantity Measured	Test
SiO2	Layer stress	Wafer curvature
Comb	Geometry	SEM
Comb	Elastic modulus	Cantilever deflection
Comb	Layer stress	Vernier gage
Comb	Resonant frequency	Dynamic test
Al	Sheet resistivity	Kelvin probe
Al	Adhesion	Square test structures

Layer stress is often an extremely important parameter in the manufacture of microelectromechanical systems. Layer stresses can affect layer adhesion, uniformity and structural integrity, among other things. For this reason, the layer stress present in the oxide and comb layers is of interest. Perhaps the simplest method for calculating layer stress is the wafer curvature test. For a uniform layer, the wafer profile may be used to calculate layer stress (σR) using the relation [11]:

$$\sigma_R = \frac{1}{6}\left[\frac{E}{1-\nu}\right]\frac{h^2}{H}\kappa \quad , \qquad (8)$$

where E is the substrate elastic modulus, ν is the Poisson ratio of the substrate material, h is the substrate thickness and H is the film thickness. Wafer curvature (κ) is given by:

$$\kappa = \frac{8B}{L^2} \quad , \qquad (9)$$

where B is the maximum deflection of the center of the wafer and L is the length of the profilometer scan. While the employment of the wafer curvature test is rather simple, it cannot be accurately determine the stress in patterned layers. As a result, this test will be used to measure layer stress in the oxide layer only. The method of determining stress in the comb layer will be described later in this report.

Another relatively simple characterization step is the measurement of device dimensions using scanning electron microscopy (SEM). SEM images of a device provide extensive information

concerning device geometry and materials. In this study, SEM will be used to measure comb dimensions and locate defects.

Due to the inevitability of material property variation with process parameters and the pronounced effect that material properties may have on the success or failure of a device, it is important to test the properties of a deposited material. For the application presented in this paper, the elastic modulus modulus (E) is an important parameter since it will be used to calculate the comb layer stress. The elastic modulus will also affect the natural frequency of the variable capacitor. While various methods for measuring E in a thin film exist, one particularly simple method was chosen in which the deflection of a cantilever test structure is measured (Fig 6).

$$F = \frac{wt^3 d}{4L^3}\frac{E}{(1-\nu)} \qquad (10)$$

Where F is the contact force and d is the tip deflection [12]. It is anticipated that measurements of deflection as a function of distance along the beam may be obtained using a profilometer by moving the stylus (which presses down on the beam with the specified contact force) along the length of the beam. Once the elastic modulus of the comb layer has been determined, the layer stress may be calculated.

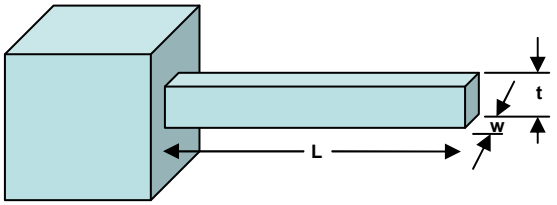

Figure 6. Schematic of a cantilever beam test structure used to calculate the elastic modulus of a thin film.

The resonant frequency of the comb is an important parameter since the scavenged energy will be at a maximum when the comb frequency matches the source frequency. Using these measurements, we will be able to make adjustments to the shuttle mass, such that the natural frequency is equal to the design value of 120Hz. The procedure for measuring resonant frequencies proposed by Smith et al [13] may be used to accomplish this task.

In order to measure intrinsic stresses in non-planar layers, a Vernier gage will be used. Vernier gages are useful since a single structure is capable of providing a quantitative measurement of both compressive and tensile stress. A Vernier gage is essentially two offset, fixed beams which are joined in the center by a "pointer" beam (Fig. 7). By measuring the deflection of the pointer beam, the layer stress may be calculated from the tip deflection (d).

$$\sigma_R = \frac{1}{E}\frac{O \cdot d}{(L_A + L_B)(L_C + \frac{1}{2}O)}, \qquad (11)$$

where E is the elastic modulus of the layer and all other parameters are as indicated in figure 7. While the method for determining film stress presented in this paragraph is effective, it is also important to note that several other test structures may be used to make the same measurement.

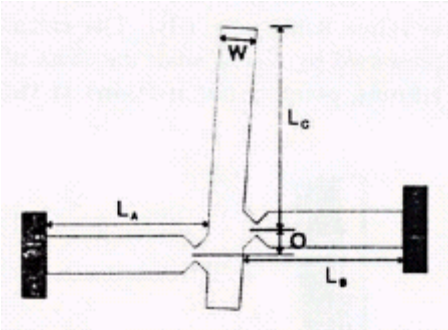

Figure 7. Vernier gage schematic showing dimensional parameters [14].

Another important process parameter that will be tested is layer adhesion. The test structures shown are capable of qualitatively testing layer adhesion as a function of contact surface area (Fig 8). Essentially, the test pattern reveals the minimum dimensions which will allow a given layer to adhere to the substrate. The smallest square which adheres to the substrate will be quite obvious following development since the structures which do not adhere fall off of the substrate and their absence indicates that the adhesion of the layers was not sufficient to hold the structure. Therefore, this test will show the critical dimensions for the adhesion of a structural layer. Incidentally, this structure will also be useful in determining if etch holes for release structures are necessary and how large they should be. While circular structures could also be used for this test, square structures were chosen because they are expected to better represent the major driving force behind delamination in the comb capacitor. Specifically, stress concentrations in sharp corners are expected to be the predominant cause of layer delamination.

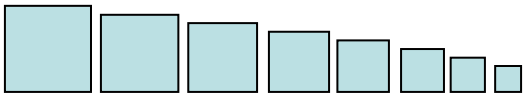
Figure 8. Layer adhesion and release test structures.

Fabrication:
The challenge when designing a micromechanical electrostatic energy converter is providing a large enough capacitance to allow effective energy conversion. The capacitance is proportional to the area of the fingers and inversely related to the gap between them. Therefore, the capacitance can be increased by either increasing the thickness of the device or decreasing the gap between the fingers. The limit to which one can adjust these parameters is dependant upon the fabrication technique. Using high aspect ratio processes, including deep reactive ion etching, thick features with narrow gaps can be fabricated. Prior designs have used this technique to build silicon based devices with aspect ratios greater than twenty.

The Utah Microfabrication Facility is not currently equipped for this process. As an alternative the device layer was fabricated using a polymeric photoresist (SU8 2025, MicroChem, San Jose,

CA). This technique has been used to design device features with moderate aspect ratios (≈2-5) and steep side walls. Using SU-8 to form comb drive structures is an untested process. We were initially concerned that the strength of the SU-8 resist would lead to device spring or comb finger failure. Ultimately, it was excessive surface stresses (≈ 1GPa) that lead to the catastrophic failure of the device during the release step.

In future designs we recommend the use of a high aspect Si compatible DIRE process when fabricating the comb structures. Using this process, features with aspect ratios (≈ 20) significantly greater than what is capable with an SU-8 process can be achieved. A proposed fabrication process is outlined below (Figure 9). The process parameters are untested but may provide a starting point for future students.

Step 1. A SOI (100) wafer contains the substrate, sacrificial and feature layers. The feature layer is typically between 25 and 50 um thick.

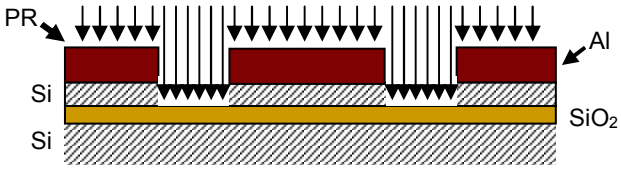

Step 2. Apply and pattern phtoresist mask, and DRIE top silcon layer

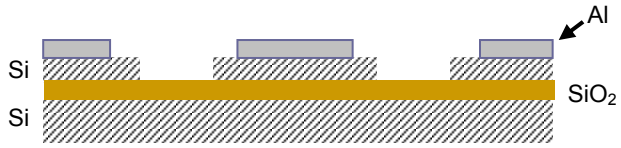

Step 3. Deposit aluminum metallization layer with a shadow mask.

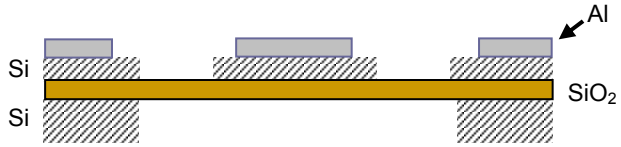

Step 4. Perform backside etch (KOH) to remove portions of the handle wafer

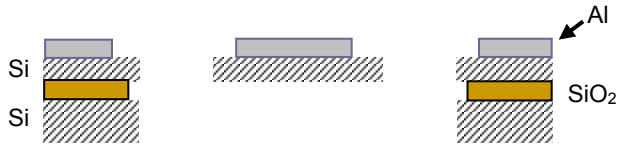

Step 5. A timed buffered oxide etch is used to release the feature layer structures.

Figure 9. DRIE based comb drive fabrication process.

Conclusions and Recommendations:

This project described in this report was selected by the authors in Fall of 2003 as part of the coursework requirements for their IGERT fellowship and training. Although substantial project progress was expected during the first two semesters, this was unfortunately not the case. As a result, much of the design and all of the fabrication and characterization work needed to be accomplished in the third semester. Fortunately, with a multidisciplinary team now in place, it was possible to accelerate our progress by concurrently addressing design, fabrication, and characterization issues. This approach did lead to a preliminary design with a compatible fabrication process which incorporated several in-line characterization test structures. Feedback from these test structures was intended to not only evaluate our process, but also provide empirical material properties that would provide feedback to the design simulations.

Ultimately the fabrication process was unsuccessful and the performance of the device could not be evaluated. There was clearly several breakdowns within the material properties, structure and processing triangle. To generate the needed capacitance the structure of the device consisted of long (3mm) slender (15um) and relatively thick (45um) comb fingers. There are only a handful of processes capable of producing features with this type of geometry. We were limited in the number of processes that we could accomplish in the Utah Microfabrication Facility, which drove us towards the SU-8 process. The numerous bake cycles used during SU-8 processing lead to severe residual stresses. This property intrinsic to SU-8 and most likely all thin polymer layers ultimately doomed the device performance.

For any future students who are interested in this device or similar devices, we have proposed a Si compatible fabrication process The process parameter are untested but may provide a starting point for future students. However, to allow for this process a DRIE system would need to be purchased. Additionally, it would have been helpful if the capabilities of the Utah Microfabrication Facility were well understood during the initial design stages of the project. However, we still believe the microfabricated energy scavenging system would make an ideal senior or graduate level design project. The system combines aspects from several engineering disciplines and offers a great opportunity for students to execute design, simulation, fabrication and testing in a multidisciplinary group setting.

References:

1. S. Roundy, R. K. Wright, and J. Rabaey, “A study of low level vibrations as apower source for wireless sensor nodes,” Computer Communications, vol. 26, pp. 1131-1144, 2003.
2. M. Stordeur, I. Stark, Low power thermoelectric generator-self sufficient energy supply for micro systems, 16th International Conference on Thermoelectrics (1997) 575–577.
3. T. Starner, Human-powered wearable computing, IBM Systems Journal 35 (3) (1996) 618–629.

N.S. Shenck, J.A. Paradiso, Energy scavenging with shoe-mounted piezoelectrics, IEEE Micro 21 (2001) 30–41.

4. A. Mehra, X. Zhang, A.A. Ayon, I.A. Waitz, M.A. Schmidt, C.M. Spadaccini, A six-wafer combustion system for a silicon micro gas turbine engine, Journal of Microelectromechanical Systems 9 (4) (2000) 517–526.

5. S. Roundy, P. K. Wright, J. M. Rabaey, "Energy Scavenging for Wireless Sensor Networks: With Special Focus on vibration," Kluwer Academic Publishers, 2004.
6. S. Roundy, "Energy Scavenging for Wireless Sensor Nodes with a Focos on Vibration-to-Electricity Conversion," http://engnet.anu.edu.au/DEpeople/Shad.Roundy, 2/19/2003.
7. C.B. Williams, R.B. Yates, Analysis of a micro-electric generator for microsystems, Proceedings of the Transducers 95/Eurosensors IX (1995) 369–372.
8. R. Amirtharajah, A.P. Chandrakasan, Self-powered signal processing using vibration-based power generation, IEEE Journal of Solid-State Circuits 33 (1998) 687–695.
9. S. Meninger, J. O. Mur-Miranda, R. Amirtharajah, A. P. Chandrakasan, and J. H. Lang, "Vibration-to-Electric Energy Conversion," IEEE Transactions on VLSI Systems, vol. 9, pp. 64-76, February 2001.
10. V.T. Srikar, S.M. Spearing, "A Critical Review of Microscale Mechanical Testing Methods Used in the Design of Microelectromechanical Systems," Experimental Mechanics, Vol. 43, No. 3, (2003) pp. 238-247.
11. F. E. H. Tay, J. A. Kan, F. Watt, W. O. Choong, "A Novel Micro-Machining Method for the Fabrication of Thick-Film SU-8 Embedded Micro-Channels," Journal of Micromechanics and Microengineering, Vol. 11, (2001) pp. 27-32.
12. N.F. Smith, D.M. Tanner, S.E. Swanson, S.L. Miller, "Non-Destructive Resonant Frequency Measurement on MEMS Actuators," in 39th Annual International Reliability Physics Symposium. Orlando, Florida, 2001, pp. 99-105.
13. B.P. van Drieenhuizen, et. al, "Comparison of Techniques for Measuring Both Compressive and Tensile Stress in Thin Films," Sensors and Actuators A, Vol. 37-38, (1993) pp. 756-765.
14. M. Boutry, A. Bosseboeuf, G. Coffignal, "Characterization of Residual Stress in Metallic Films on Silicon with Micromechanical Devices," Proceedings of the SPIE, Vol. 2879, (1996)